Statistical Properties Of Dark Matter Halos From Cosmological Simulations

Project Report

Submitted by

Mr. Albin P James
Reg. No: M200591PH

In partial fulfillment of the award of the degree of

MASTER OF SCIENCE
IN
PHYSICS

Under the supervision of

Dr Charles Jose
Assistant Professor
Department of Physics, CUSAT

Department Of Physics
National Institute of Technology, Calicut
May 2022

DECLARATION

I hereby declare that this submission is my own work and that, to the best of knowledge and belief, it contains no material previously published or written by any other person nor material which has been accepted for the award of any other degree or diploma of the university or other institute of higher learning, except where due acknowledge has been made in the text.

Albin P James
MSc Physics
Reg No: M200591PH
Department of Physics
NIT Calicut

CERTIFICATE

This is to certify that the project report entitled **"Statistical Properties Of Dark Matter Halos From Cosmological Simulations"** submitted by **Mr Albin P James** (**Roll No: M200591PH**) to National Institute of Technology Calicut, towards partial fulfillment of requirements for the award of Degree of Master of Science (Physics) is a bona fide record of project work done by him under my supervision.

Supervisor
Dr Charles Jose
Assistant Professor
Department of Physics
CUSAT, Kochi

Internal Supervisor
Dr P N Bala Subramanian
Assistant Professor
Department of Physics
NIT Calicut

Project Coordinator
Dr Goutam Kumar Chandra
Assistant Professor
Department of Physics
NIT Calicut

Head of the Department
Dr Aji A Annappara
Associate Professor
Department of Physics
NIT Calicut

ACKNOWLEDGEMENT

This project owes its culmination, in the present form, due to the support, guidance and help that I received from several sources. The success of this study is the result of the cooperation of various people.

I deem it a pleasure to express my deep obligation to my project guide Dr Charles Jose, Assistant Professor, Department of Physics, Cochin University of Science and Technology, for his sincere guidance and insightful suggestions in preparing this project work. I will always be indebted for the knowledge and work experience he has instilled in me.

I extend my sincere thanks to Dr Aji A Anappara, Head of the Department of physics, my internal guide Dr P N Bala Subramanian, faculty advisor Dr Goutam Kumar Chandra, the entire faculty and non-teaching staff of the Department of Physics for their kind support and valuable guidance throughout my work.

I want to utilise this opportunity to thank all the data sources (AbacusSummit) for providing me with their valuable data to complete this work. I also thank the faculty in charge and staff of the High-Performance Computing facility at NIT Calicut for allowing me to use the MADHAVA HPC Cluster for my computational needs.

Last but not least, I extend my sincere thanks to my parents, family and classmates for their deep encouragement and support.

Albin P James
MSc Physics
Reg No: M200591PH
Department of Physics
NIT Calicut

ABSTRACT

In the theory of cosmological structure formation, galaxies form in gravitationally bound dark matter clumps called dark matter halos. In this project, we investigate the statistical properties of dark matter halos using numerical simulations. In particular, we estimate the halo mass function, which is the number density of dark matter halo as a function of mass, for various redshifts and box sizes. Further, a counts-in-cells analysis for halo mass function was conducted for redshifts 0.2 and 3 by dividing the boxes into smaller boxes of 50, 25 and 20 MPc/h and measuring the variation of mass function across sub boxes.

Keywords: Halo Mass function, HMF, Counts-In-Cells, Statistical Properties, Dark Matter Halos

Contents

List of Figures

Chapter 1

Cosmology

Cosmology is the study of large scale properties of the universe. The cornerstone of modern cosmology is the assumption that the place we occupy is in no way unique, called the cosmological principle. According to the cosmological principle, the universe on a large-scale possess two properties, Homogeneity: The universe looks the same at each point and Isotropy: The universe looks the same in all directions (Liddle, 2015).

1.1 ΛCDM: The Concordance Model

Our expanding universe has a flat geometry and consists of visible baryonic matter, Cold Dark Matter (CDM) and the cosmological constant denoted by Λ. Currently, all measurements point to dark energy being the cosmological constant Λ. Moreover, inflation explains the initial perturbations of the structure formations in the early universe. This concordance model is known as the flat Λ CDM model.

1.1.1 Dark Matter

Our observations show that dark matter outweighs visible matter roughly six to one, making up about 24% of the universe. Observational abnormalities such as galactic rotation curves and velocities of galaxies in galactic clusters led to the detection of the presence of these invisible components known as Dark Matter.

The rotation curve measures the velocity of stars or galactic gas as a function of distance from the centre of the galaxy. The velocities increase beyond the distance where visible matter is present, and the curve flattens off. On the contrary, Kepler's laws predict the velocities to decrease rapidly. This flattening indicated the presence of extra mass, which is not visible.

In clusters, galaxies have more velocities than what the gravitational force can balance. Kinetic energy must balance the potential energy. In order for the clusters to be stable, there must be more mass than what is visible (De Swart et al., 2017)

Even though invisible, they are crucial in explaining many observed phenomena because of their large quantity. One such phenomenon is the formation of large scale structures. Matter, both ordinary and dark, together evolve from gravitational, and overdense regions collapse to form structure in the universe.

1.1.2 Dark Energy

Dark energy is the component of matter responsible for the universe's accelerated expansion. They form about 72% of the universe. Unlike dark matter, they do not cluster strongly. Einstein first introduced the idea of the cosmological constant, which he later abandoned.

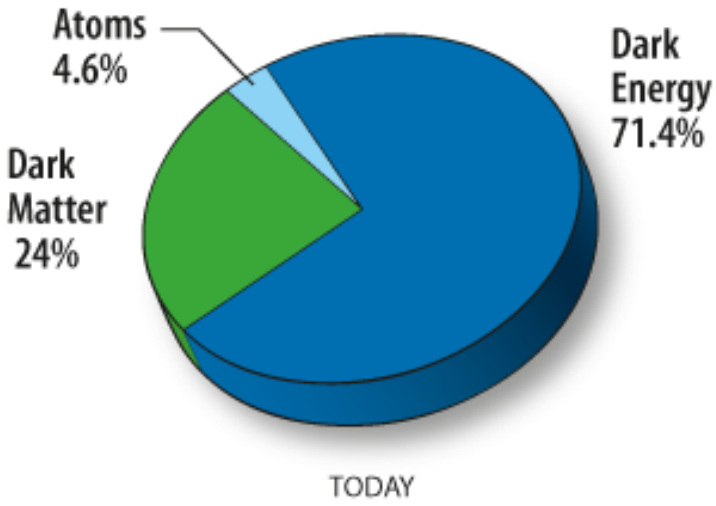

Figure 1.1: Pie chart represneting the content of our universe (NASA, 2013).

1.1.3 Baryons

Baryons are the visible component of matter in the universe. They form about 5% of the total matter in the universe. Stars are made up of baryons. They are particles which constitute three quarks. Of all possible baryons, only protons and neutrons can only be stable. We are all comprised of atoms. These protons and neutrons contribute to the bulk of the mass. Electrons are also included under this label by cosmologists.

1.2 Large Scale Structures

The cosmological principle speaks about how the universe is homogeneous and isotropic. However, at small scales, this assumption breaks and there exists inhomogeneities. These inhomogeneities gravitationally evolve to form the present matter distribution consisting of galaxies and clusters. As the majority of the mat-

ter is dark matter, the evolution of the matter density field and hence the large scale structures are highly influenced by it (Cooray and Sheth, 2002).

1.2.1 Dark Matter Halos

They are gravitationally bound dark matter only regions. As perturbations in dark matter collapse under gravity, virialisation happens, i.e. the kinetic energy of the dark matter particles will get balanced by the gravitational potential from halos. When gravitational collapse occurs, they will only oscillate about the centre of mass to finally relax to form halo-like regions (Mo et al., 2010).

The Halo model says that galaxies form inside the potential well provided by the halos. All galaxies are hosted by a dark matter halo of some mass, and converse may not hold as low mass halos may not host galaxies (Dodelson and Schmidt, 2020). Even clusters form inside associated halos.

1.2.2 Halo Mass Function

The halo mass function (HMF) is the statistical property of cosmological structure formation models, which gives the number density of haloes as a function of mass.

One can directly measure the HMF from the simulations. We can also theoretically predict it using the halo model of large scale structures.

Chapter 2

N Body Simulations

2.1 Introduction

The observations of our vast universe tell us it is composed mainly of enormous structures like galaxies and clusters of galaxies. We currently explain the formation of these enormous structures as due to the gravitational amplification of small perturbations.

Gravity is the dominant force driving the growth of these small perturbations into large dense systems with a matter density thousand times larger than the average density of the universe. We assume gravity as the only interaction possible for the growth of perturbations at large scales. For tiny density differences and highly symmetric circumstances, analytical solutions to the equations describing the evolution of density perturbations in non-relativistic matter due to gravitational interactions are possible. They help to understand the universe's evolution in the quasi-linear regime, and these fail when density contrast becomes large.

In the absence of analytical methods for computing quantities of interest, numerical simulations are the only tool available to study clustering in the non-linear regime (Bagla and Padmanabhan, 1997). Along with it in galactic scales, gas dynamics and other effects play an important role and need to be considered for a detailed solution to the problem.

Equations to evolve the density perturbations have been known for a long time (Peebles, 1974) and can solve quickly when the amplitude of perturbations is small. These equations evolve the density contrast, given by

$$\delta(\vec{r}, t) = (\rho(\vec{r}, t) - \bar{\rho}(t))/\bar{\rho} \tag{2.1}$$

Where $\rho(\vec{r}, t)$ is the density at point $\vec{r}$ in time t, $\bar{\rho}$ denotes the average density of the universe.

The densities here describe non-relativistic matter concentrations which can cluster at all scales and are the driving force behind the construction of large-scale structures in the cosmos. When the density contrast at relevant scales is high, i.e. $|\delta| \geq 1$, the perturbation becomes non-linear. In this regime, the evolution equations cannot be solved for generic perturbations, and hence N-Body Simulations are used (Bagla, 2005, Bagla and Padmanabhan, 1997, Bertschinger, 1998, Springel and Hernquist, 2003).

A representative portion of the cosmos is simulated in cosmological N-Body simulations. As the universe is vast but finite volume, we utilise periodic boundary conditions frequently. We assume the simulation volumes to be of cubical structure in most cases. We ignore the effect of perturbations at scales smaller than the simulation's mass resolution, as is the effect of perturbations at scales larger than the box (Bagla and Prasad, 2006).

An N-body code comprises two main modules: one computes the force field for a particular particle configuration, and the other moves the particles in that force field. These two are invoked at each step to ensure that the force field and particle paths evolve in a self-consistent manner. In addition, we must set up the initial circumstances and write the output. The flow chart 2.1 depicts the basic plan of an N-Body code.

2.2 Applications of Simulations

The wide range of uses of N-Body codes includes

- Comparison of the predictions of specific dark matter models obtained from simulations with observations.
- Running simulations with initial conditions that have little to do with our universe.
- Testing approximate solutions for the growth of density perturbations by validating these approximations and determining whether they are helpful by comparing them to N-Body simulations.
- Generating mock catalogues by N-Body simulations to calibrate algorithms for analysing observations.

We can test whether a method works or not using N-Body Simulations because all the specifics are known, although this is not the case in the real universe (Bagla and Padmanabhan, 1997).

Simulations of systems, like the globular clusters, can be considered (relatively) isolated systems. In the case of Cosmological Simulations, our cosmos does not have a boundary. As a result, cosmological simulations must use periodic boundary conditions.

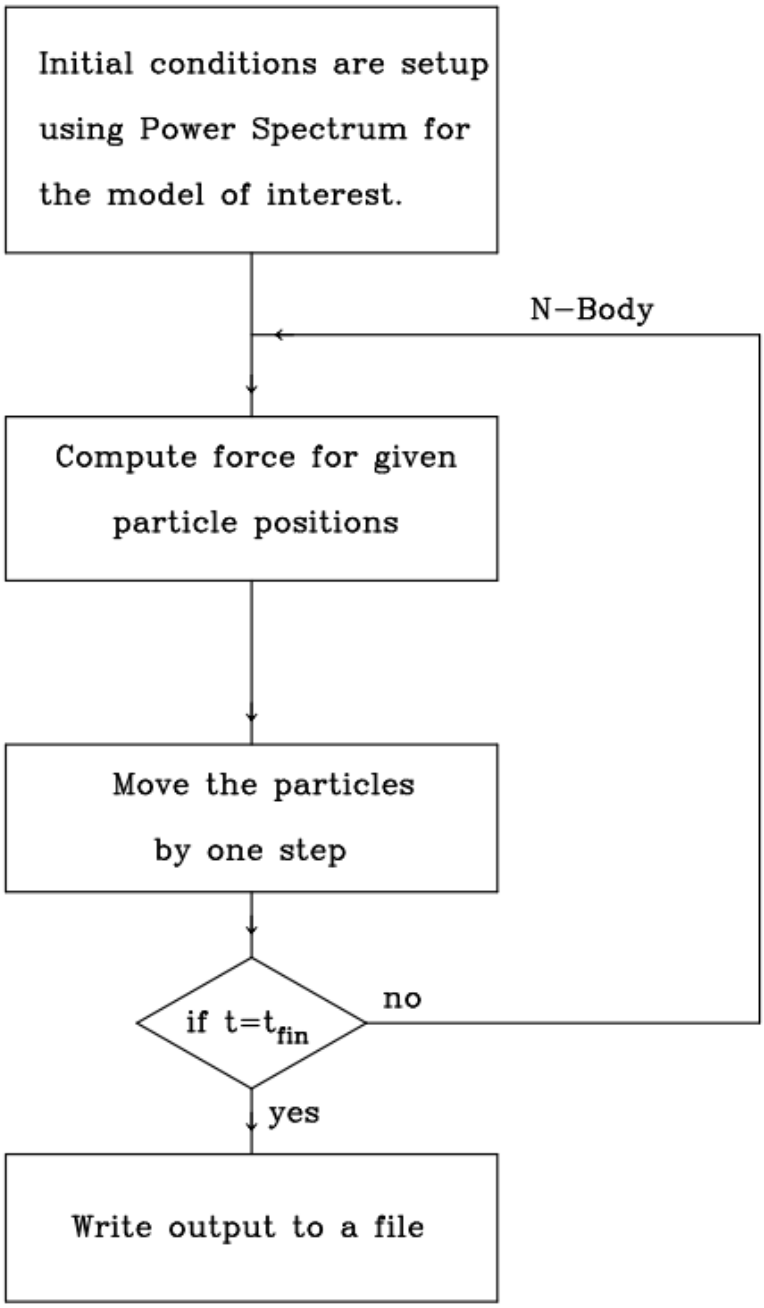

Figure 2.1: Flow chart of N-Body Code. (Bagla and Padmanabhan, 1997)

The density perturbations are there at all scales. Its amplitude is large at small scales and drops down as it goes into larger scales. Unless to research large-scale structures at early times when the amplitude of fluctuations is modest, scales more than 100MP/c are not relevant for structure formation. Hence for the study of structure formation at galactic scales, the physical size of the simulation boxes should be at least 100 MPc.

If we want to analyse the distribution of galaxies in depth, The mass of each particle should be significantly lower than the mass of a typical galaxy. Combining these two restrictions means that we need to use at least 10^8 particles in the cosmological N-Body Simulations.

Chapter 3

Statistical Properties

The previous chapter gives a general introduction to Cosmological N-Body Simulations. Here we estimate the halo mass function and analyse the dark matter halos' counts-in-cells distribution.

This study analyses data from the AbacusSummit simulation suite (Maksimova et al., 2021). We use the HFMcalc (Murray et al., 2013) tool to compute the theoretical values of the halo mass function for comparing with the value obtained from the simulation.

3.1 AbacusSummit Simulation

AbacusSummit is a suite of highly accurate cosmological simulations produced with the abacus code (Garrison et al., 2021) on the Summit supercomputer at the Oak Ridge National Laboratory.

It comprises 150 simulation boxes that span 97 cosmological models, the majority

Description	Symbol	Value
Baryon density parameter	Ω_b	0.02237
Dark matter density parameter	Ω_c	0.1200
Hubble parameter	h	0.6736
Amplitude of primodial curvature perturbations	$10^9 A_s$	2.0830
Density perturbation spectral index	n_s	0.9649
Density perturbation amplitude	σ_8	0.807952

Figure 3.1: Paramters of AbacusSummit Simulation

of which contain 330 billion particles with a mass of $2 * 10^9 h^{-1} M_\odot$. It also gives re-simulation data at lower mass resolution for resolution studies and prototyping and 1883 smaller boxes at the base resolution for statistical error evaluation. The suite contains about 60 trillion particles in total. The data outputs publically provided include full particle snapshots, particle subsamples, halo catalogues, particle lightcones, projected density maps, and particle IDs for creating high-accuracy halo merger trees (Maksimova et al., 2021).

For halo group finding, it uses a hybrid of Friends-of-friends(FoF) and Spherical Overdensity(SO) Algorithm dubbed as the CompaSO (Hadzhiyska et al., 2022).

For the study, we use the simulations with the following specifications.

1. Box Size: *base* (2000 MPch^{-1})
    - Cosmology: *Plank 2018* ΛCDM
    - Number of particles: 6912^3
    - Redshifts: 0.1, 0.2, 3
2. Box Size: *small* (500 MPch^{-1})
    - Cosmology: *Plank 2018* ΛCDM
    - Number of particles: 1728^3
    - Redshifts: 0.2, 0.5, 1.1, 2, 3

These data are analysed to study the statistical properties, including the halo mass function and the counts-in-cells.

3.2 Mass Function From N-Body Simulations

To compute the halo mass function from simulation, first, we compute the histogram by properly binning the halo based on its mass. As the mass ranges from $10^{10}h^{-1}M_{\odot}$ to $10^{15}h^{-1}M_{\odot}$, it is convenient to use the logarithmic scale. We then divide the histogram by the width of the logarithmic bin and the volume of the simulation box. We compute the mass function as

$$n(M) = \frac{N_{\ln(M)}}{V\delta(\ln(M))} \tag{3.1}$$

Where the $N_{\ln(M)}$ is the number of halos in the logarithmic bin centred at $\ln(M)$, V the volume of the simulation box and $\delta(\ln(M))$ the width of the logarithmic bins.

Below are the halo mass functions computed for various redshifts for a box of 500 MPc/h and 2000 MPc/h.

In figure 3.2 and 3.3 we show the halo mass functions computed from simulations of different box sizes and also at different redshifts in blue dots. The lines are the mass function computes using the HFMcalc tool (Murray et al., 2013).As one can see, the analytical predictions and measurements from simulations agree very well at all mass ranges and redshifts.

3.2.1 500 MPc/h Box

Simulation: AbacusSummit
Cosmology: Planck2018 LCDM

Box Length: 500 $\frac{MPc}{h}$

Particle Mass:$2.1 \times 10^9 \frac{M_\odot}{h}$

Number Of Mass Bins: 100

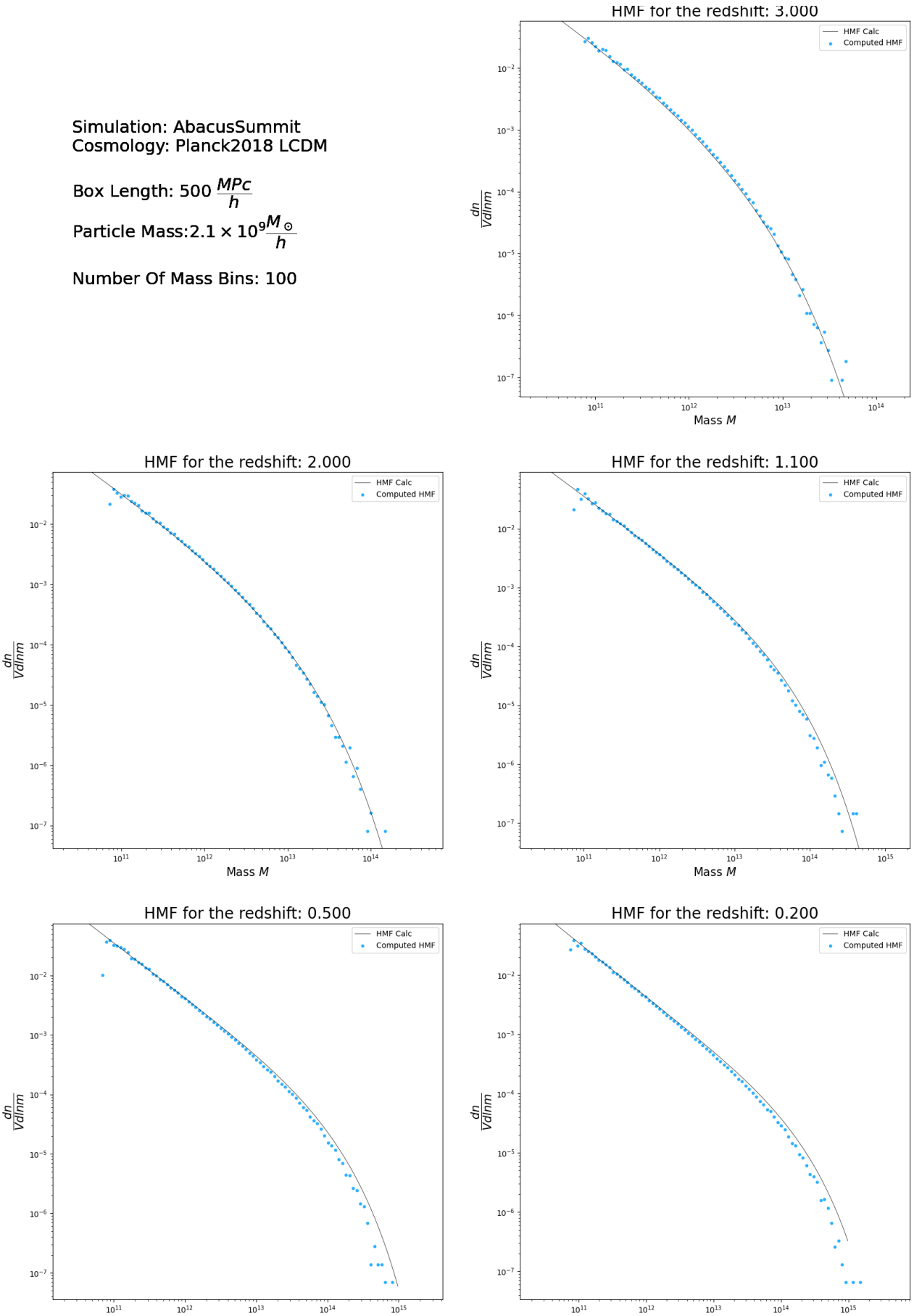

Figure 3.2: HMF for various redshifts obtained from simulation data of box side length 500 MPc/h

3.2.2 2000 MPc/h Box

Simulation: AbacusSummit
Cosmology: Planck2018 LCDM

Box Length: 2000 $\frac{MPc}{h}$

Particle Mass:$2.1 \times 10^9 \frac{M_\odot}{h}$

Number Of Mass Bins: 100

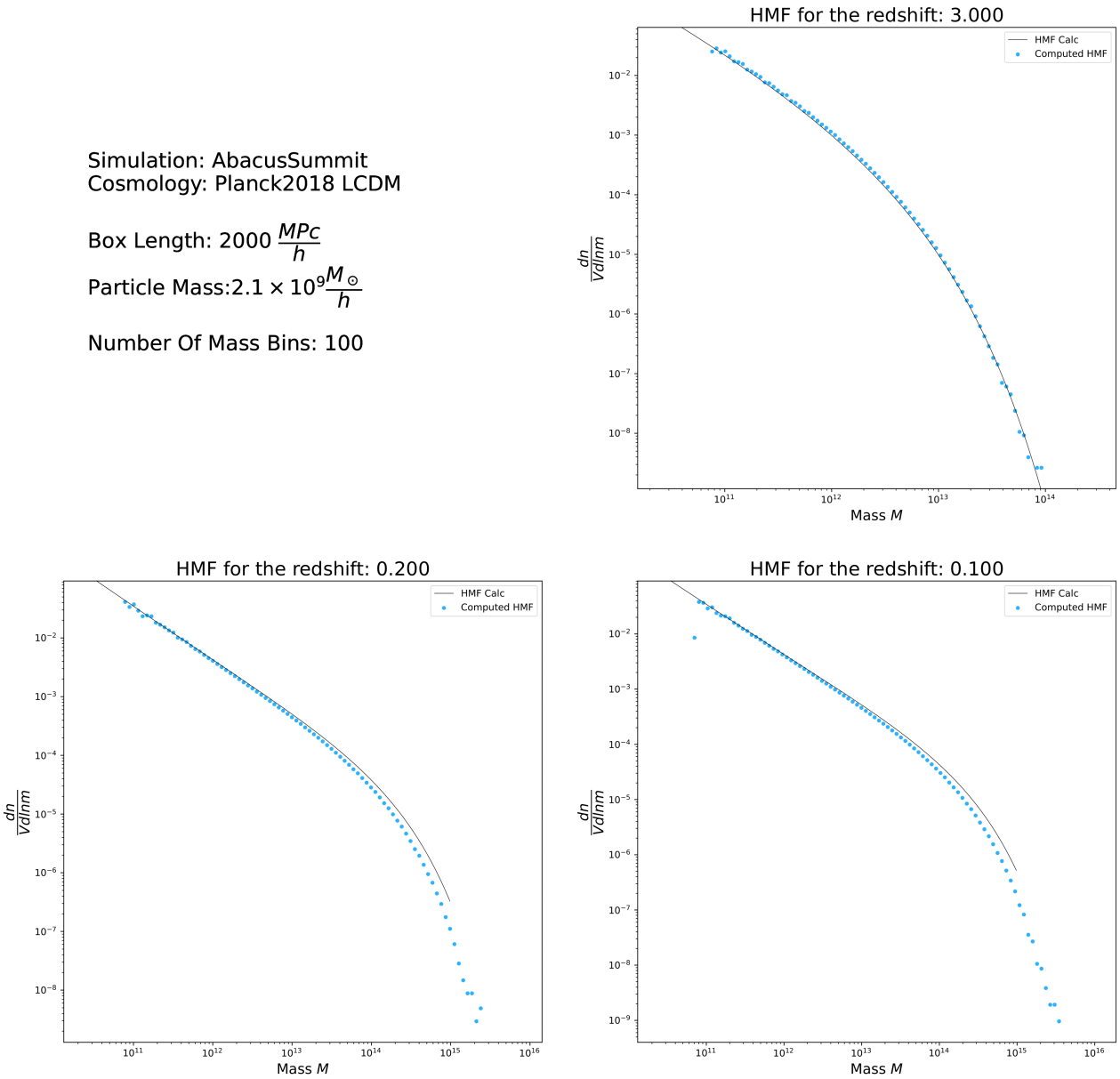

Figure 3.3: HMF for various redshifts obtained from simulation data of box side length 2000 MPc/h

3.3 Counts-In-Cells Analysis

The counts-in-cells distribution gives the probability of finding N objects in a region of space with volume V. It is obtained by analysing cells of a fixed size, either in 3D space or in projection, over a region in space by counting the number of galaxies that are within the cell (Foo et al., 2014, Rahmani et al., 2009).

For computing counts-in-cells we have divided the cubic simulations into smaller boxes of side length 50 MPc/h 3.3.1, 25 MPc/h 3.3.2 and 20 MPc/h 3.3.3 and for larger box sixes 500 MPc/h and 2000 MPc/h.

For each subvolume, we plotted the histogram for the number of dark matter halos in each subvolume. After normalising the histogram, we calculated the mean and standard deviation of the number of halos of a mass range in the sub boxes using standard python packages (Using the mean and standard deviation, we computed a normal distribution. Also, using the mean, Poisson distribution curve is calculated). The Gaussian and Poisson distributions are overplotted along with the counts-in-cells.

In the figures 3.4 to 3.12, the first plot shows the hmf as calculated in section 3.2 and lines denote the mass ranges selected for counts-in-cells analysis. The histogram plotted as explained above is shown in blue, the Gaussian distribution with dotted lines and Poisson with the solid line.

We can observe the following trends for various sub-box sizes at the two redshifts and box sizes.

- For 50 MPc/h boxes 3.3.1 we can see at mass range $10^{11} M_{\odot}$ to $10^{12} M_{\odot}$, it follows the Gaussian distribution closely and at $5 \times 10^{12} M_{\odot}$ we can see it shifitng to Poisson distribution.

- In 25 MPc/h boxes 3.3.2 we can see at mass $10^{11} M_{\odot}$ it follows the Gaussian distribution closely, and at $5 \times 10^{11} M_{\odot}$ and above, we can see it shifting to Poisson distribution.

- Finally, in the 25 MPc/h boxes 3.3.2 we can see at mass $10^{11} M_{\odot}$ it slowly shift from the Gaussian distribution, and as mass increases, it agrees to the Poisson distribution.

3.3.1 50 MPc/h Boxes

Simulation: AbacusSummit
Cosmology: LCDM
Redshift: 3.000
Box Length: 500 MPc/h

Sub Box Length: 50.0 MPc/h
Total Number Of Sub Boxes: 1000

Number Of Mass Bins: 100

Number of halos: 3346751

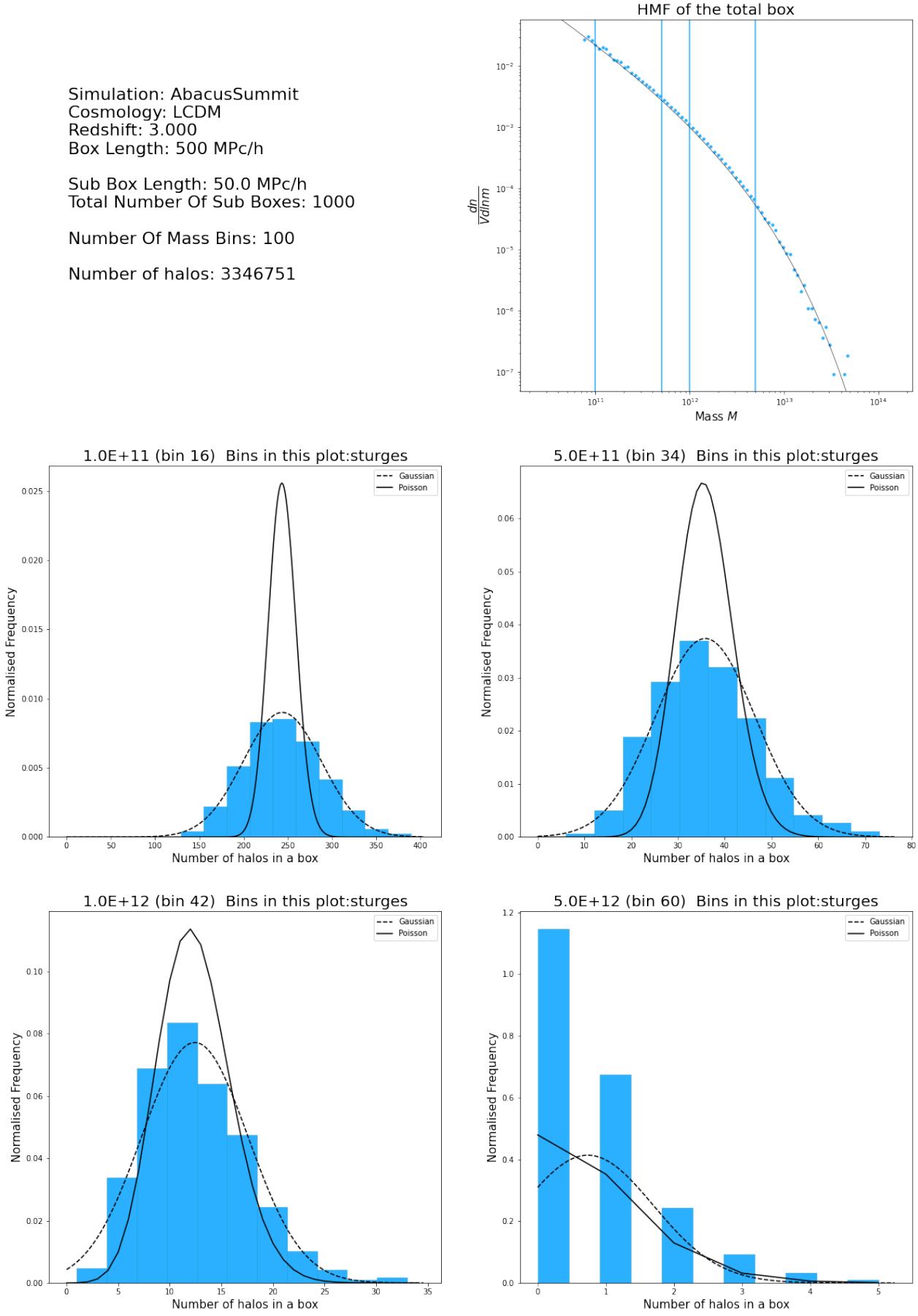

Figure 3.4: Halo number frequency distribution obtained from simulation data of box side length 500 MPc/h at z=3 by dividing it into box of side 50 MPc/h

Simulation: AbacusSummit
Cosmology: LCDM
Redshift: 3.000
Box Length: 2000 MPc/h

Sub Box Length: 50.0 MPc/h
Total Number Of Sub Boxes: 64000

Number Of Mass Bins: 100

Number of halos: 215026242

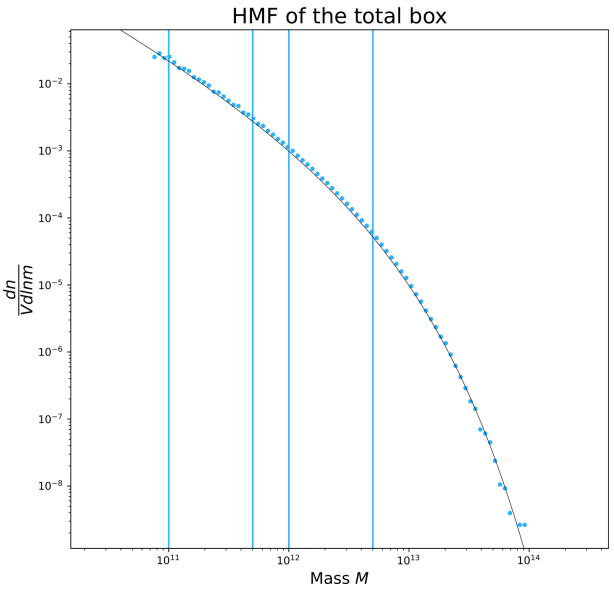

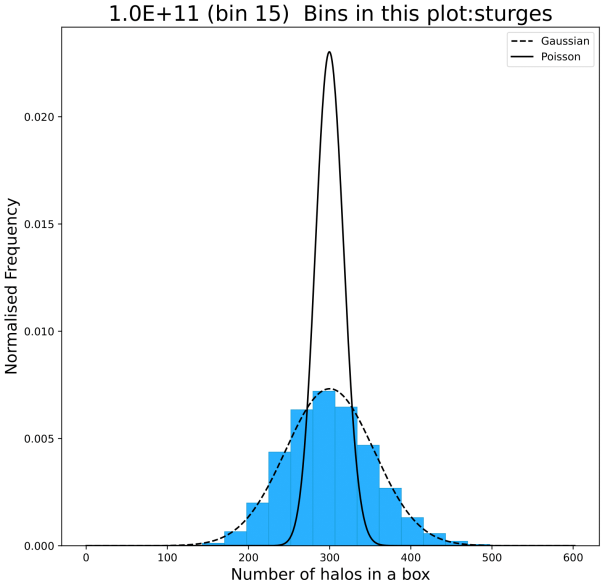

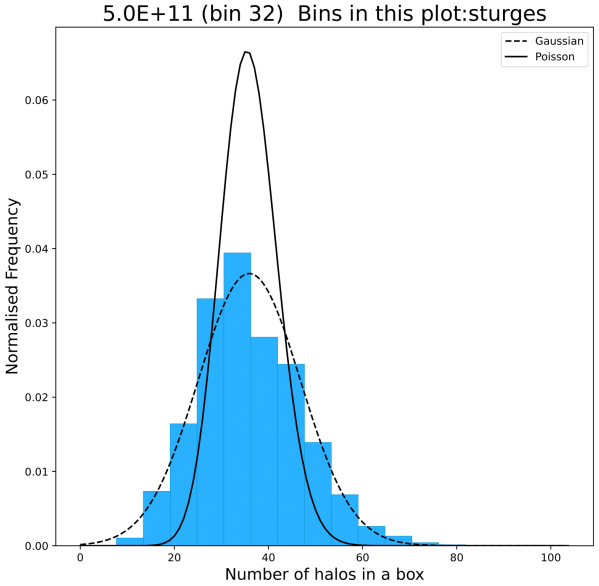

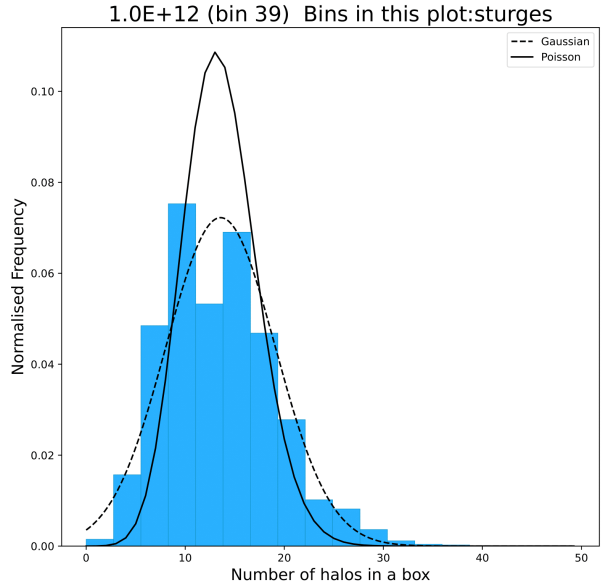

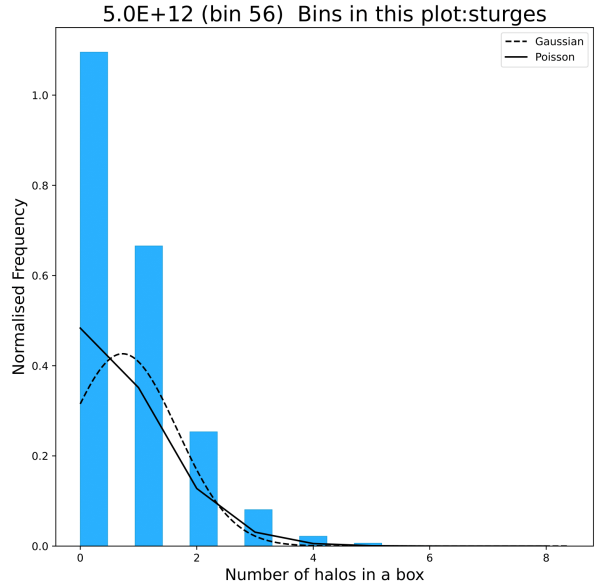

Figure 3.5: Halo number frequency distribution obtained from simulation data of box side length 2000 MPc/h at z=3 by dividing it into box of side 50 MPc/h

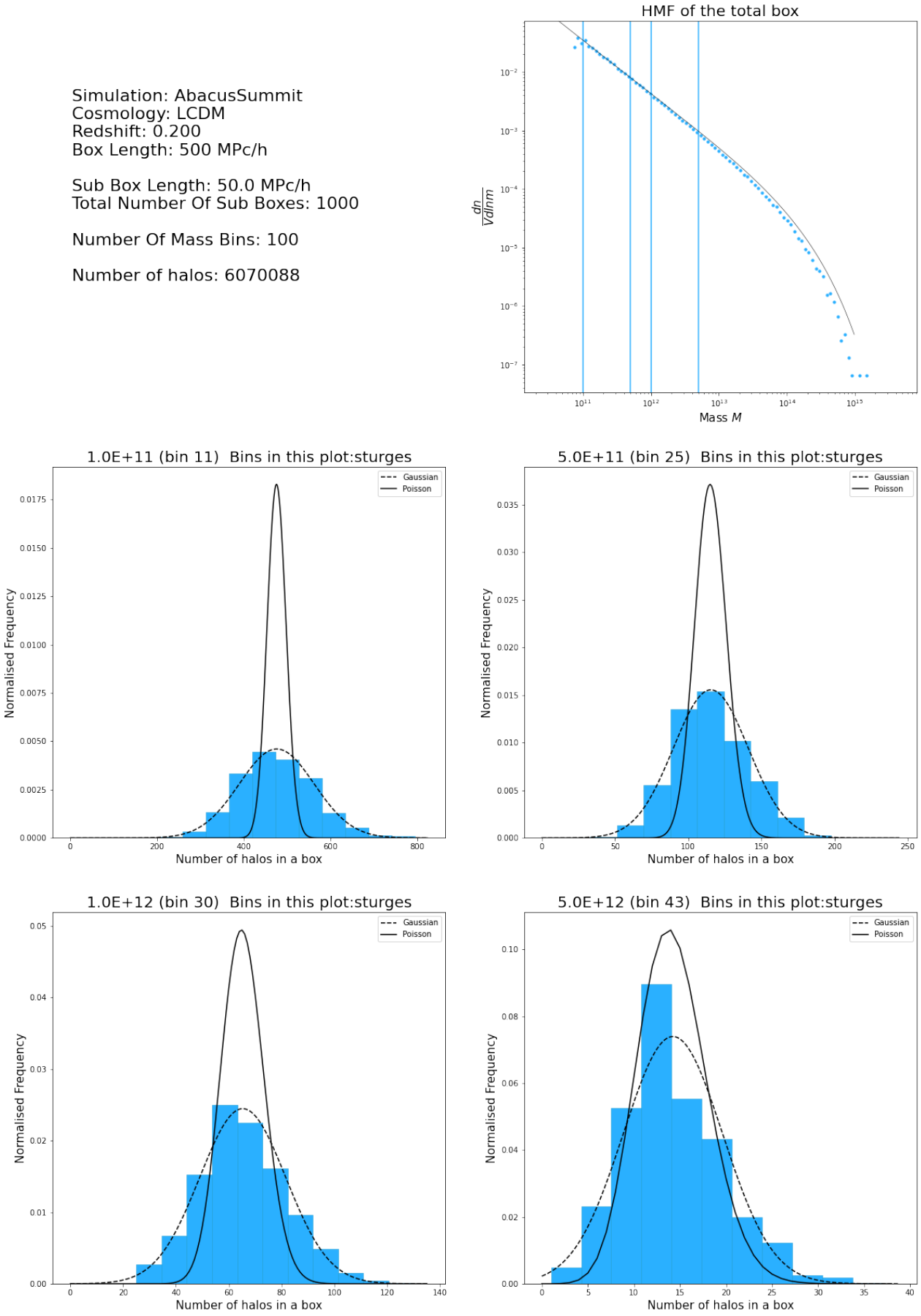

Figure 3.6: Halo number frequency distribution obtained from simulation data of box side length 500 MPc/h at z=0.2 by dividing it into box of side 50 MPc/h

3.3.2 25 MPc/h Boxes

Simulation: AbacusSummit
Cosmology: LCDM
Redshift: 3.000
Box Length: 500 MPc/h

Sub Box Length: 25.0 MPc/h
Total Number Of Sub Boxes: 8000

Number Of Mass Bins: 100

Number of halos: 3346751

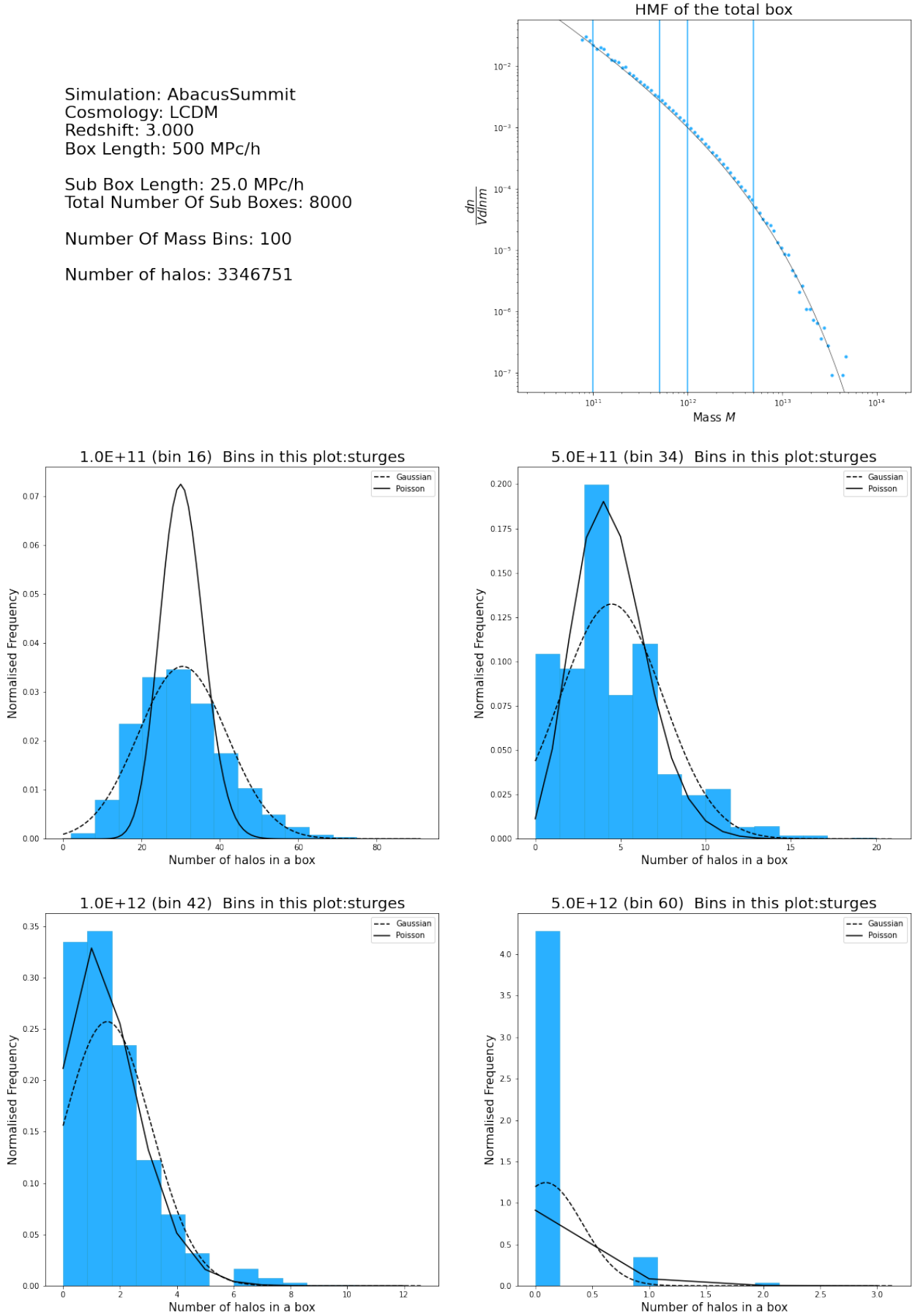

Figure 3.7: Halo number frequency distribution obtained from simulation data of box side length 500 MPc/h at z=3 by dividing it into box of side 25 MPc/h

Simulation: AbacusSummit
Cosmology: LCDM
Redshift: 3.000
Box Length: 2000 MPc/h

Sub Box Length: 25.0 MPc/h
Total Number Of Sub Boxes: 512000

Number Of Mass Bins: 100

Number of halos: 215026242

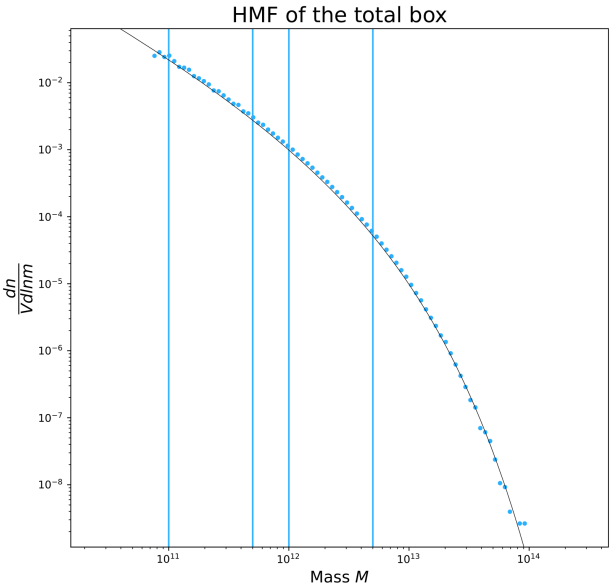

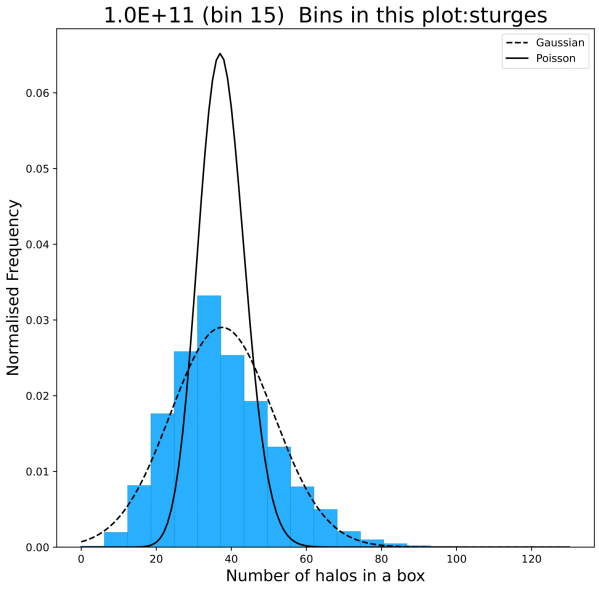

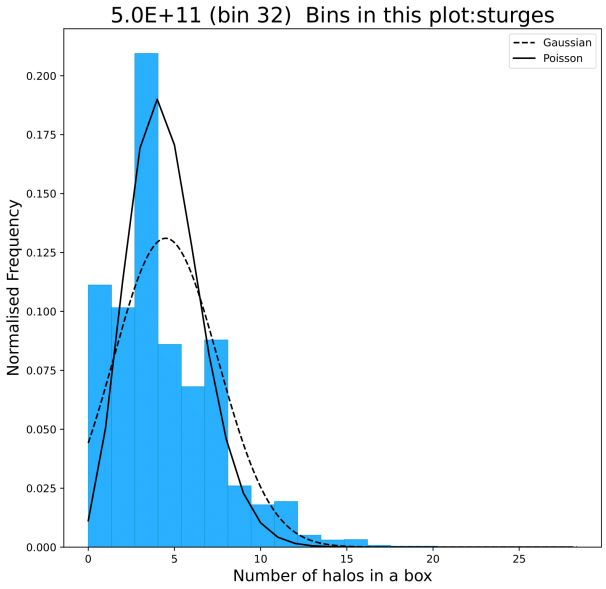

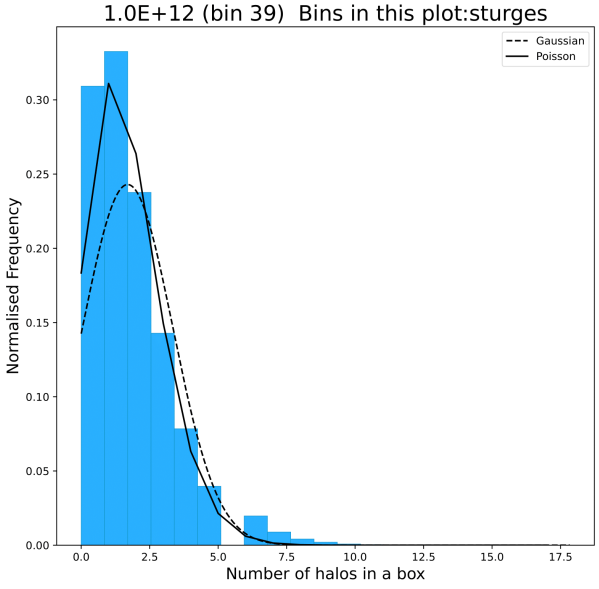

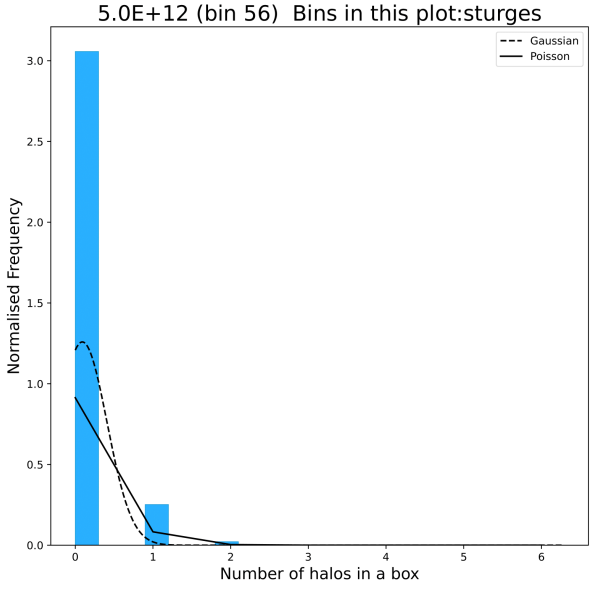

Figure 3.8: Halo number frequency distribution obtained from simulation data of box side length 2000 MPc/h at z=3 by dividing it into box of side 25 MPc/h

Simulation: AbacusSummit
Cosmology: LCDM
Redshift: 0.200
Box Length: 500 MPc/h

Sub Box Length: 25.0 MPc/h
Total Number Of Sub Boxes: 8000

Number Of Mass Bins: 100

Number of halos: 6070088

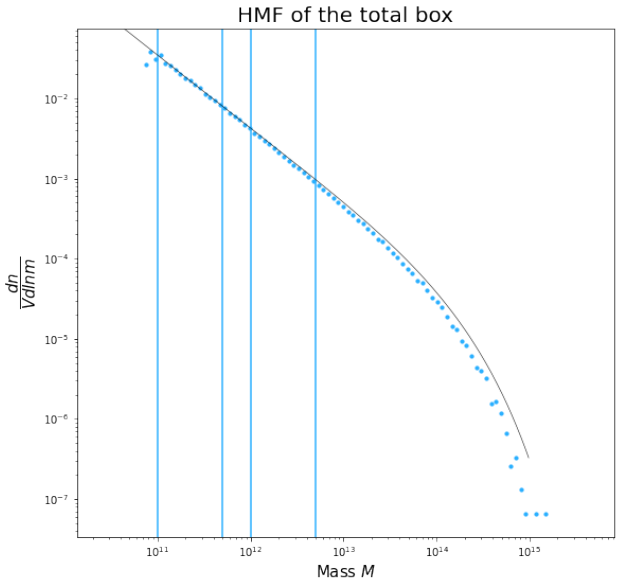

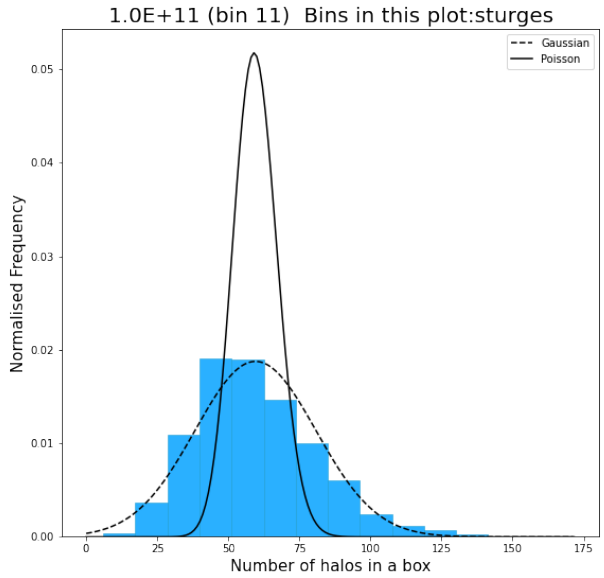

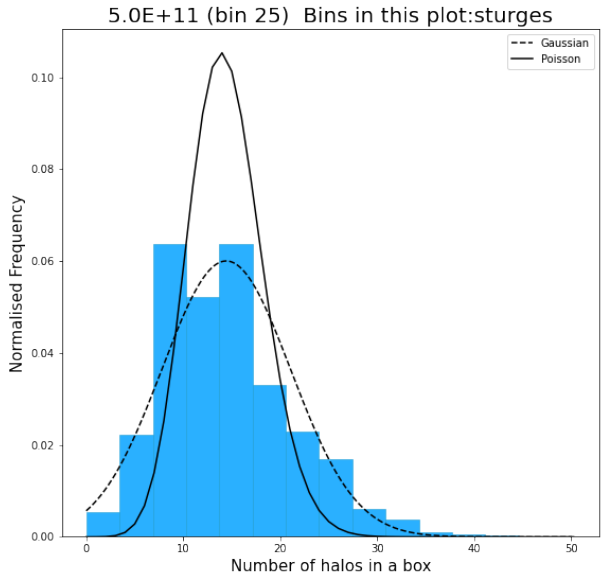

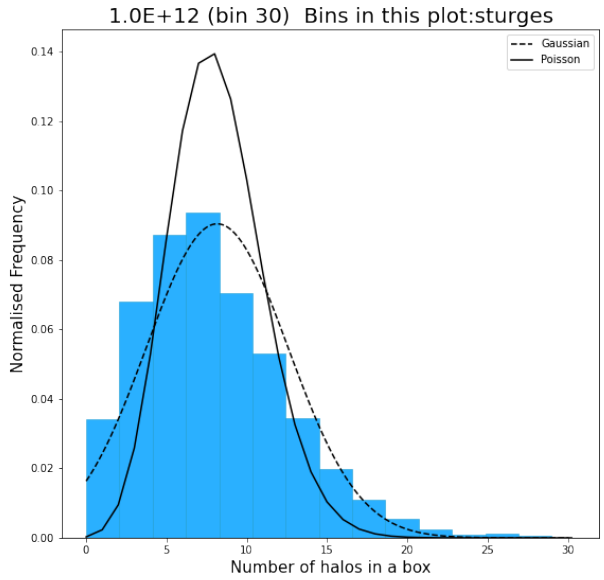

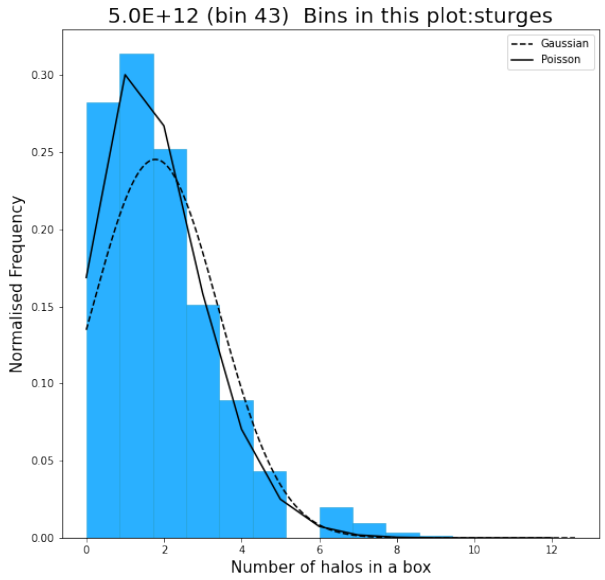

Figure 3.9: Halo number frequency distribution obtained from simulation data of box side length 500 MPc/h at z=0.2 by dividing it into box of side 25 MPc/h

3.3.3 20 MPc/h Boxes

Simulation: AbacusSummit
Cosmology: LCDM
Redshift: 3.000
Box Length: 500 MPc/h

Sub Box Length: 20.0 MPc/h
Total Number Of Sub Boxes: 15625

Number Of Mass Bins: 100

Number of halos: 3346751

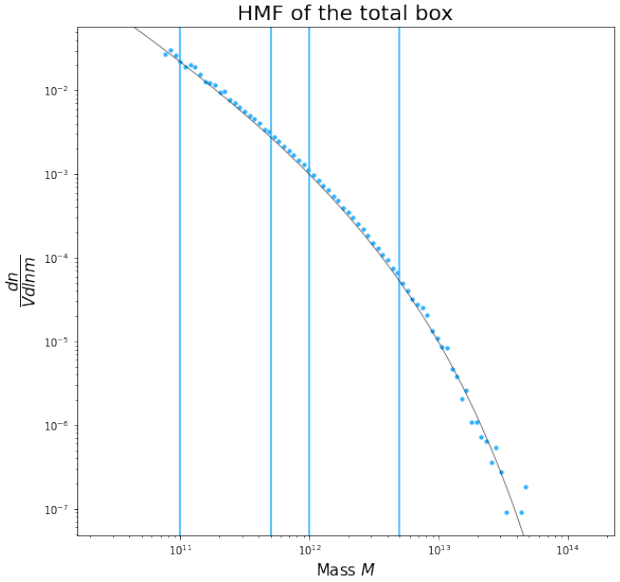

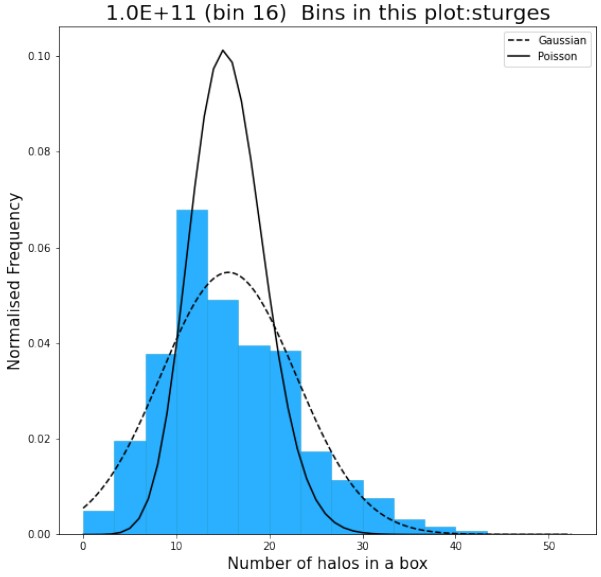

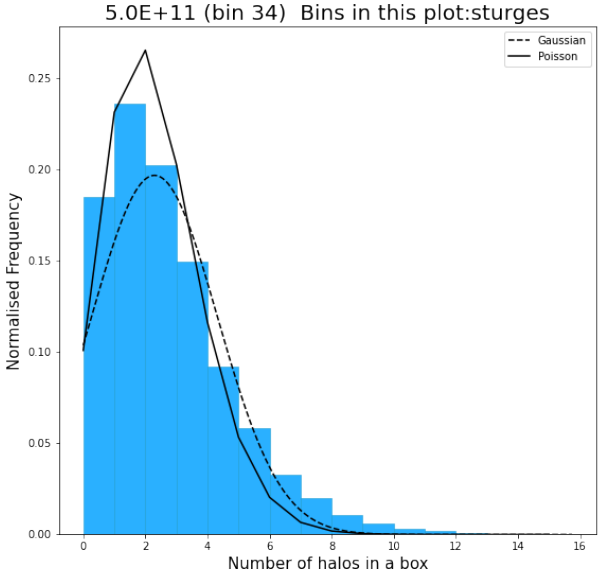

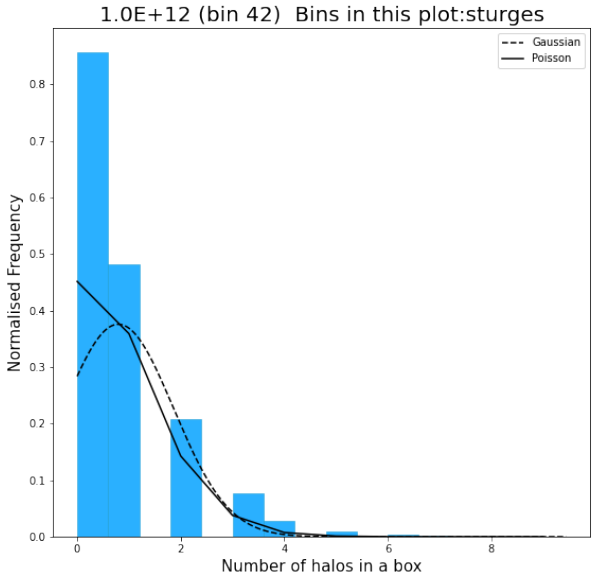

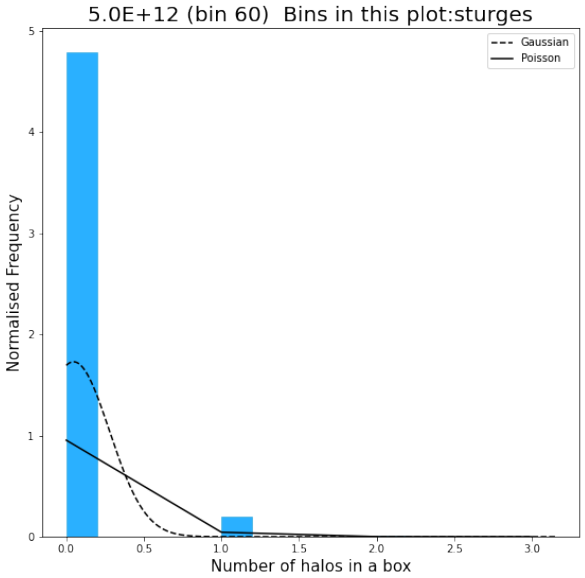

Figure 3.10: Halo number frequency distribution obtained from simulation data of box side length 500 MPc/h at z=3 by dividing it into box of side 20 MPc/h

Simulation: AbacusSummit
Cosmology: LCDM
Redshift: 3.000
Box Length: 2000 MPc/h

Sub Box Length: 20.0 MPc/h
Total Number Of Sub Boxes: 1000000

Number Of Mass Bins: 100

Number of halos: 215026242

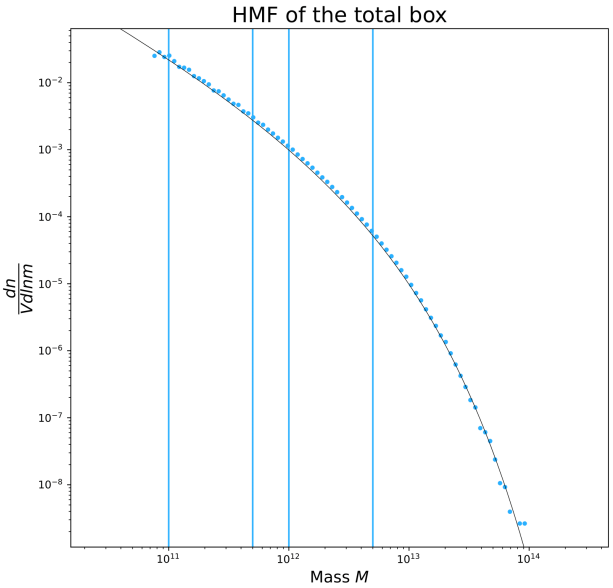

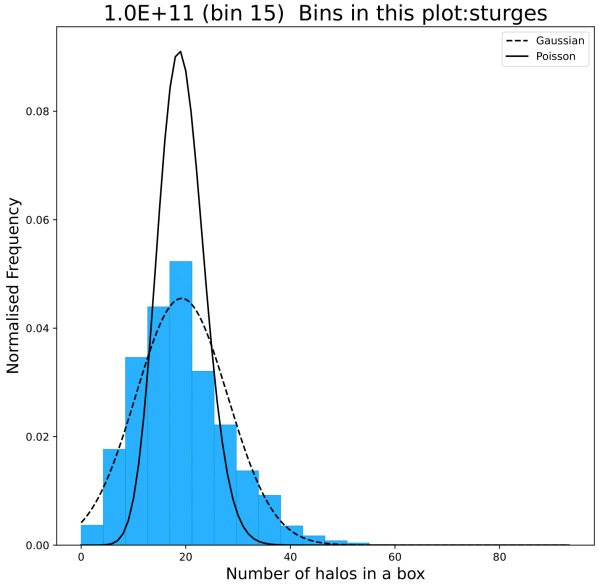

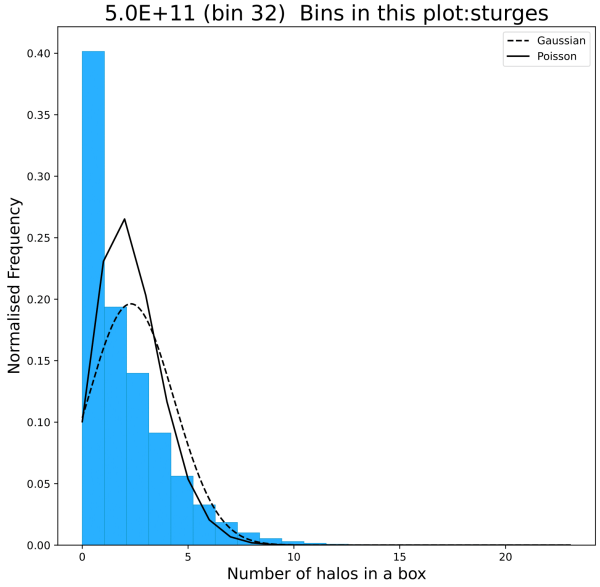

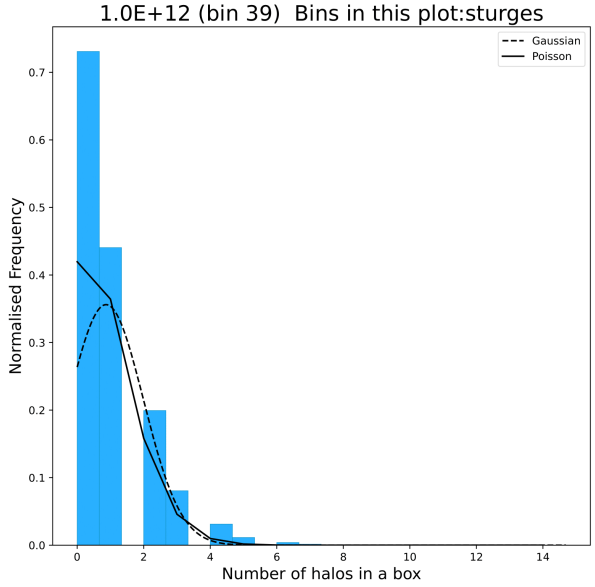

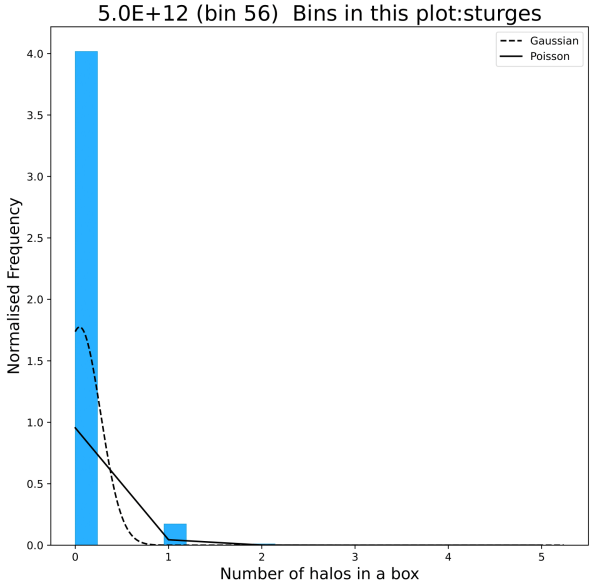

Figure 3.11: Halo number frequency distribution obtained from simulation data of box side length 2000 MPc/h at z=3 by dividing it into box of side 20 MPc/h

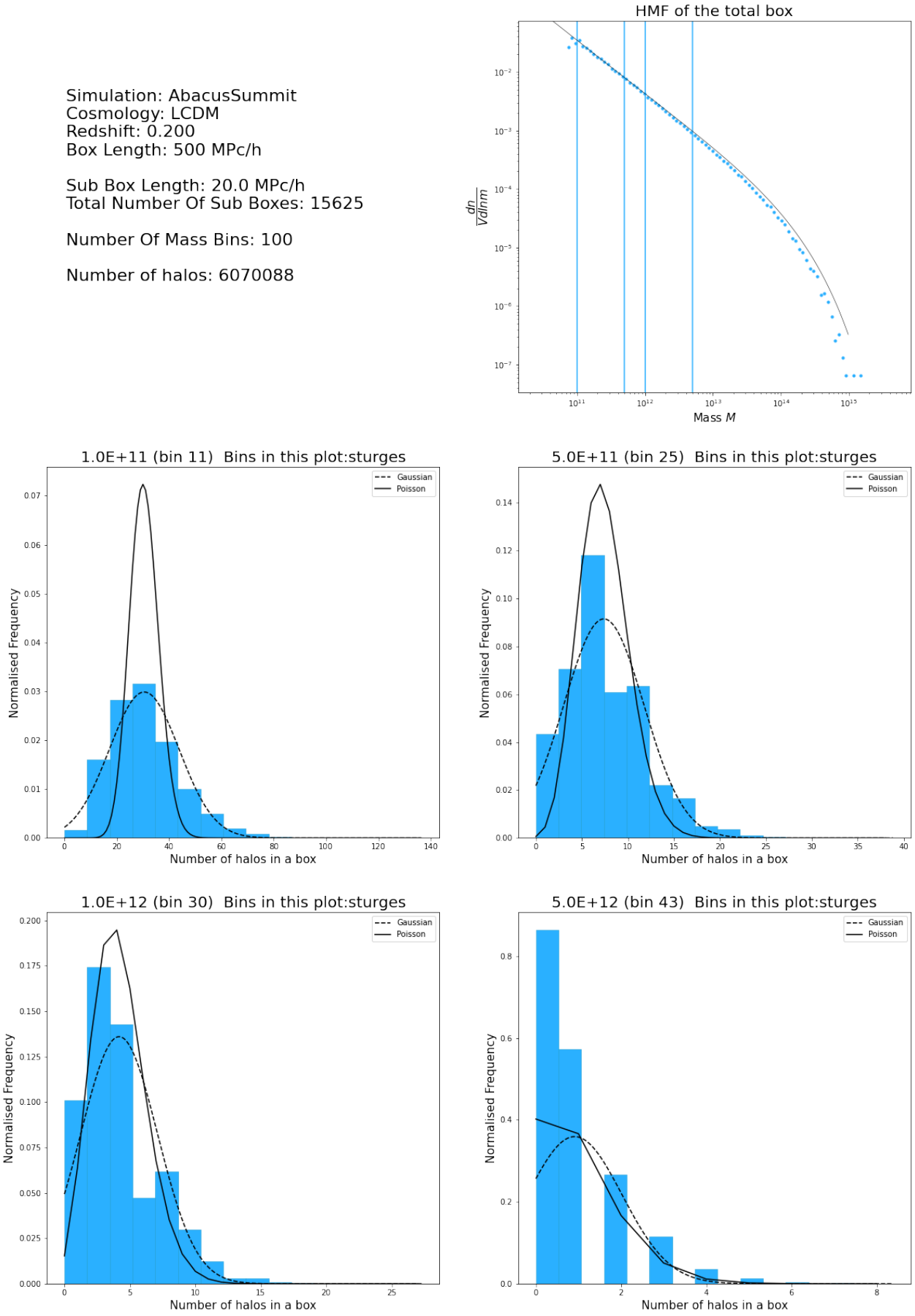

Figure 3.12: Halo number frequency distribution obtained from simulation data of box side length 500 MPc/h at z=0.2 by dividing it into box of side 20 MPc/h

Chapter 4

Conclusion

In this project we have studied the statistical properties of dark matter halos, namely its halo mass function and have conducted counts-in-cells for halo mass function in sub boxes using numerical simulation data.

For computing the halo mass function as described in session **??**, we have used the data from the AbacusSummit simulation. We computed the HMF for box sizes 500 MPc/h and 2000 MPc/h for various redshifts. We could see considerable agreement, especially in the lower mass regions, when we compared this data with analytically generated HMF (using the HMFCalc tool). As the mass increases, we see a considerable deviation from the values calculated using the HMFCalc tool.

We have also conducted the counts-in-cells analysis as described in session 3.3. The Gaussian and Poisson distribution curves were calculated and overplotted over the histogram, using the mean and standard deviation of the number of halos in sub boxes. As explained in session 3.3, we could see that for all the sub-box sizes computed, at masses close to $10^{11} M_{\odot}$, it follows the Gaussian distribution curve

pattern. However, we found a shift from normal to Poisson distribution curve pattern as we increased the mass range.

Appendix A

Links to the Data and Code

To obtain the data and various codes in this study the following URLs were used.

- The AbacusSummit simulation data: https://abacusnbody.org/
- AbacusSummit doumentation: https://abacussummit.readthedocs.io/en/latest/
- Python package abacusutils: https://github.com/abacusorg/abacusutils
- The code developed for this study: https://github.com/albinpjames/SParkHalos

Bibliography

Bagla, J. and Prasad, J. (2006). Effects of the size of cosmological n-body simulations on physical quantities–i. mass function. *Monthly Notices of the Royal Astronomical Society*, 370(2):993–1002.

Bagla, J. S. (2005). Cosmological n-body simulation: Techniques, scope and status. *Current science*, pages 1088–1100.

Bagla, J. S. and Padmanabhan, T. (1997). Cosmologicaln-body simulations. *Pramana*, 49(2):161–192.

Bertschinger, E. (1998). Simulations of structure formation in the universe. *Annual Review of Astronomy and Astrophysics*, 36(1):599–654.

Cooray, A. and Sheth, R. (2002). Halo models of large scale structure. *Physics reports*, 372(1):1–129.

De Swart, J., Bertone, G., and van Dongen, J. (2017). How dark matter came to matter. *Nature Astronomy*, 1(3):1–9.

Dodelson, S. and Schmidt, F. (2020). *Modern Cosmology*. Elsevier Science.

Foo, F. F., Yang, A., and Chan, A. H. (2014). The high-redshift galaxy counts-in-cells from the cosmos survey. In *Proceedings Of The Conference In Honour Of The 90th Birthday Of Freeman Dyson*, pages 463–467. World Scientific.

Garrison, L. H., Eisenstein, D. J., Ferrer, D., Maksimova, N. A., and Pinto, P. A. (2021). The abacus cosmological n-body code. *Monthly Notices of the Royal Astronomical Society*, 508(1):575–596.

Hadzhiyska, B., Eisenstein, D., Bose, S., Garrison, L. H., and Maksimova, N. (2022). compaso: A new halo finder for competitive assignment to spherical overdensities. *Monthly Notices of the Royal Astronomical Society*, 509(1):501–521.

Liddle, A. (2015). *An Introduction to Modern Cosmology*. Wiley.

Maksimova, N. A., Garrison, L. H., Eisenstein, D. J., Hadzhiyska, B., Bose, S., and Satterthwaite, T. P. (2021). Abacussummit: a massive set of high-accuracy, high-resolution n-body simulations. *Monthly Notices of the Royal Astronomical Society*, 508(3):4017–4037.

Mo, H., van den Bosch, F., and White, S. (2010). *Galaxy Formation and Evolution*. Galaxy Formation and Evolution. Cambridge University Press.

Murray, S. G., Power, C., and Robotham, A. S. (2013). Hmfcalc: An online tool for calculating dark matter halo mass functions. *Astronomy and Computing*, 3:23–34.

NASA (2013). Content of the universe - pie chart.

Peebles, P. (1974). The effect of a lumpy matter distribution on the growth of irregularities in an expanding universe. *Astronomy and Astrophysics*, 32:391.

Rahmani, H., Saslaw, W. C., and Tavasoli, S. (2009). The spatial distribution function of galaxies at high redshift. *The Astrophysical Journal*, 695(2):1121.

Springel, V. and Hernquist, L. (2003). Cosmological smoothed particle hydrodynamics simulations: a hybrid multiphase model for star formation. *Monthly Notices of the Royal Astronomical Society*, 339(2):289–311.